

Power Density and Efficiency Optimization of Resonant and Phase-Shift Telecom DC-DC Converters

U. Badstuebner, J. Biela and J. W. Kolar
 Power Electronic Systems Laboratory, ETH Zurich
 ETH-Zentrum, ETL H12, Physikstrasse 3
 CH-8092 Zurich, Switzerland
 Email: badstuebner@lem.ee.ethz.ch

Abstract—Power density and efficiency are one of the major driving forces in the development of new power supplies for telecommunication and information industry. The phase-shift PWM and the series-parallel resonant DC-DC converter are promising topologies that can meet these demands at high power rates. Based on conventional criteria such as the number of semiconductors/passive components or voltage/current stress it is not possible to identify the topology that offers a higher power density or efficiency.

Therefore, an optimization procedure has been developed, which calculates the optimal converter parameters (e.g. switching frequency or transformer design) with respect to the maximal power density and/or efficiency. This procedure is based on detailed analytical models for the converter, semiconductor losses, HF losses in the magnetic components as well thermal and geometrical models of the transformer.

With the procedure a 5 kW series-parallel resonant converter and a phase shift converter with capacitive output and with current doubler have been optimized. With the calculated parameters a resonant converter prototype has been constructed and experimental results are presented.

I. INTRODUCTION

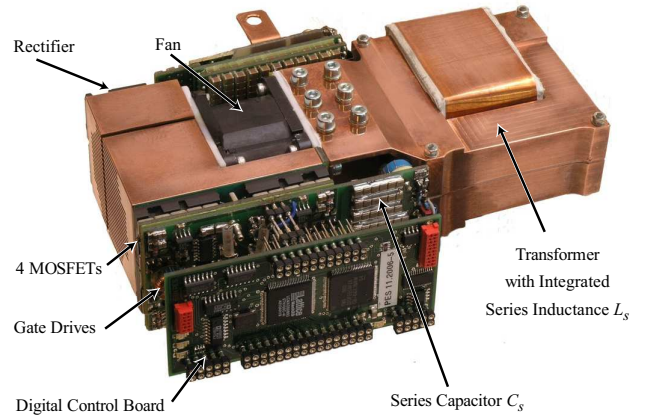
Over the last decades, a major effort in the information and telecommunication industry has been increasing the power density of the deployed power supplies in order to meet the design requirements concerning maximum weight, limited space and production costs [1]. The increasing density has been mainly enabled by the continuous development of high performance switching devices which allow a higher switching frequency at relatively low switching losses, what leads to a reduced volume of the passive components.

Besides the power density, system efficiency is a major driving force due to the continual increase of energy consumption and costs. Therefore, the development focuses now on high efficiency power supplies, which enable cost and cooling effort reduction.

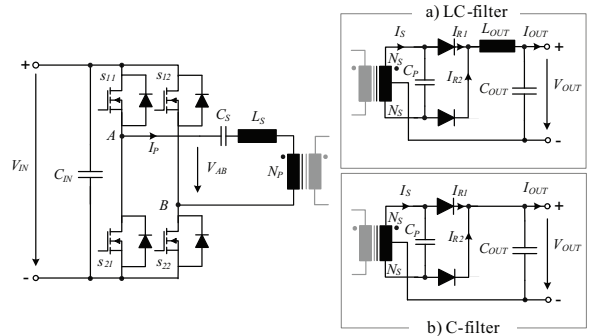
Switch mode power supplies applied in telecommunication systems and data centers typically consist of an AC-DC rectifier with power factor correction (PFC) as input stage and

Table I: Typical specifications of IT DC-DC converter.

Input voltage	V_{IN}	400 V
Output voltage	V_{OUT}	48...54 V
Output power	P_{OUT}	5 kW
Output ripple voltage	V_{ripple}	300 mV _{pp}
Max. ambient temperature	T_{amb}	45 °C



Prototype: Height: 1 U = 1.75 in \approx 44 mm, volume: 0.49 liter, power density: 167 W/in³ = 10.2 kW/liter



Schematic: a) LC-filter and b) capacitive filter as output stage

Figure 1: Prototype and schematic of a series-parallel resonant DC-DC converter, 5 kW, 400 V/48..54 V.

a DC-DC converter as output stage, which steps the DC link voltage down to the required output voltage of 48 V to 54 V. There, usually transformers, enabling a large voltage transfer ratio, are applied for galvanic isolation (e.g. [2],[3]).

The typical specifications for IT DC-DC converters are given in table I. In the literature several topologies for the rectifier and DC-DC converter have been proposed (e.g. [4][11]). A comparison of these topologies based on criteria like stress of the semiconductors, number of switches or

ZVS/ZCS condition only allows to reduce the number of topologies to a few promising ones. For a more detailed comparison identifying the most suitable topology, an optimization of each topology with respect to the considered comparison criteria, power density and efficiency, is required.

Therefore, a comparison of different DC-DC converters topologies based on an optimization procedure with comprehensive analytical models is presented in this paper. The most suitable topologies for high power telecom converters are the series-parallel resonant converter (schematic and the constructed hardware based on the optimization procedure are shown in Fig. 1) and the phase-shift PWM converter (cf. Fig. 2), which both allow soft-switching. For these two converters different output stages (LC-filter, C-filter with mid point connection and current doubler) are possible and have been investigated [12].

A short survey on applicable topologies and an evaluation, based on the mentioned criteria with respect to the achievable power density and efficiency, is given in in **Section II**. There, also the operation of the phase-shift and the series-parallel resonant converter including the digital control using a state machine is shortly explained. For the topology comparison a comprehensive optimization procedure is required, which is presented in **Section III** with the corresponding different analytical models for the converters such as the HF transformer losses and the temperature distribution.

With the presented optimization procedure the two topologies have been optimized, once for power density and once for maximum efficiency. The corresponding results of the optimization and a comparison of both converter topologies are discussed in **Section IV**. In the same section a validation of the resulting optimized parameters based on a circuit simulation is given. For validating the results a prototype and measurement results of an optimized series-parallel resonant converter are presented in **Section V**. There, also the design of a phase-shift converter with current doubler and the comparison between copper and aluminum heat sinks is given.

II. CONVERTER TOPOLOGIES FOR IT APPLICATIONS

In the area of low power converters often flyback and single switch forward converters are applied. These topologies are not suitable if high output power with high efficiency is required. Enhanced and/or other topologies proposed for telecom supplies are, for example, the double interleaved forward converter [4], [13], the asymmetrical half bridge [5] and multiresonant topologies [7]. However, these topologies do not fit the requirements concerning efficiency and high power density in the same way as full bridge topologies, operating with soft switching, due to the amount of semiconductors and passive components and/or the utilization of the duty cycle in half bridges which results in larger transformers. In addition, the switching and conduction losses in asymmetrical half bridges increase and the efficiency decreases due to the asymmetrical current waveforms at high input voltages [6].

As already mentioned in section I, the series-parallel resonant (cf. Fig. 1 bottom) and the phase-shift PWM full-bridge DC-DC converter (cf. Fig. 2) are well applicable for the considered telecom application. Both converters operates

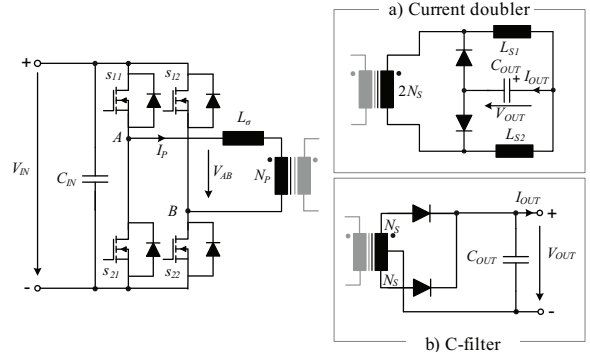


Figure 2: Schematic of a phase-shift DC-DC converter with a) current doubler or b) center-tapped transformer with LC-filter.

with soft-switching and enable high efficiency at higher output power levels. In addition, full-bridge converters better utilize the transformer due to the bipolar flux swing. Therefore, a smaller transformer size and weight can be achieved.

A. Phase-Shift PWM DC-DC Converter

When operating a conventional PWM full bridge at high power and high frequency, the converter performance will be reduced by the switching losses due to the circuit parasitics. A specially-operating mode of the PWM full bridge, allows all switching devices (cf. Fig. 2) to operate under zero voltage (ZVS) condition (e.g. in [2], [11]). There, the parasitics of the circuit are advantageously used to achieve the soft-switching condition.

In Fig. 2 two possible output stages are shown: a mid point connection with C-filter (CTC) and the current doubler (CDR). Both topologies enable a compact construction with high efficiency and will be considered in the optimization.

In Fig. 3 the control scheme and the principle voltage/current waveforms of the phase-shifted PWM converter are given. There, the power flow is controlled by the phase-shift between the two legs, which also determines the duty cycle of the converter. The switching of all four IGBTs/MOSFETs is performed under ZVS condition by using the energy stored in the leakage inductance (L_σ , cf. Fig. 2), in order to charge/discharge the parasitic output capacitances of both switches in the switching leg. Further details can be found in literature mentioned above.

B. Series-Parallel Resonant DC-DC Converter

The series-parallel resonant converter is a combination of a series and a parallel resonant DC-DC converter, as shown in Fig. 1. With a proper choice of the resonant tank components values (C_S , L_S and C_P), the series-parallel resonant converter combines the advantages of the series resonant converter:

- Series capacitor C_S blocks the DC voltage, thus avoiding the transformers saturation
- The partial load efficiency is high due to the decrease in device currents with a decrease in load

and the advantages of the parallel resonant converter:

- Controlled operation at light load

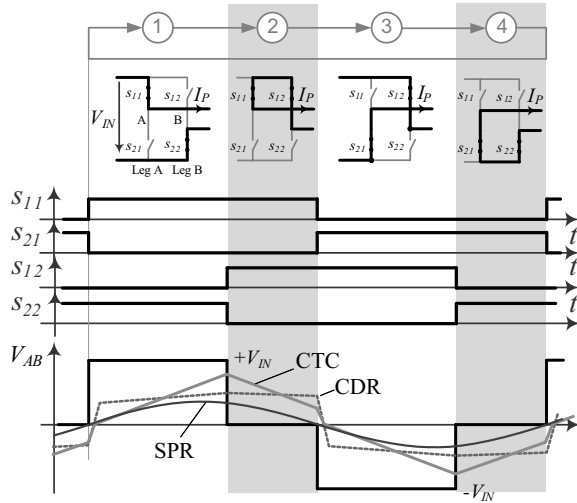


Figure 3: Switching states and current waveforms for phase-shift converter with capacitive output filter and current doubler as well as for the series-parallel resonant DC-DC converter with capacitive output filter.

while most of the disadvantages of the two converters are eliminated (e.g. [6], [9], [14]). Furthermore, the converter is naturally short circuit proof.

For a compact design, a center-tapped transformer with rectifier as output stage results in a lower volume if high output currents are required. As presented in [8], the capacitive output filter (cf. Fig. 1 b) results in a smaller volume than the LC-filter for high output currents. Therefore, the LC-filter is not considered in the following.

As the phase-shifted converter, the series-parallel resonant converter provides soft switching of all 4 switches. By controlling the zero-crossing of the resonant current I_P it is possible to achieve zero-voltage switching in one leg and zero-current switching (ZCS) in the other one.

The operation principle of the switches is similar to the phase-shifted converter as shown in Fig. 3. Due to the filtering action of the resonant circuit the primary current I_P is approximately sinusoidal, which has the benefit of better EMI performance.

As it can be seen in the schematics (Fig. 1b) and Fig. 2) and the control scheme (cf. Fig. 3), the phase-shift and the resonant converter are very similar and show almost the same performance and similar efficiency (e.g. [3]). Thus, conventional criteria are not sufficient to identify the most suitable especially in respect to minimal volume, lowest cost or highest efficiency. By means of optimizing the three converter topologies for one or even more criteria like power density and/or efficiency based on detailed models, a profound comparison based on the optimization is possible. This optimization procedure and the associated models described in the following section.

III. OPTIMIZATION PROCEDURE

For the comparison of the different topologies, the component values must be chosen, so that the power density

Table II: Constraints used for the optimization procedure ($CSPI =$ Cooling System Performance Index cf. [17]).

Max. Width	1U = 1.75 in \approx 44 mm
Core Material	N87 (EPCOS, $T_{max} \leq 115^\circ\text{C}$)
MOSFETs	APT50M75 (Mircosemi, former APT)
Rectifier Diodes	APT100S20 (Mircosemi, former APT)
Capacitors C_S and C_P	3.9 nF, 800 V, COG (NOVACAP)
$CSPI$	23
Max. Junction Temp.	$T_{j,max} \leq 140^\circ\text{C}$

and/or the efficiency becomes maximal. Since the volume of the single components, which are mainly limited by the respective maximum operation temperature, interdependent to some extent on each other, the optimization of the overall volume is a quite difficult task with many degrees of freedom. Therefore, an automatic optimization procedure is applied for determining the optimal component values of the telecom supply.

The optimization procedure is mainly based on 4 models:

- An analytical converter model, based on the extended fundamental analysis (series-parallel resonant converter, [8], [15]) and/or time domain analysis (phase-shift converter, [16]), respectively
- Equations for the semiconductor switching and conduction losses, based on measurements
- Model for the volumes of the resonant tank capacitors, including dielectric losses
- A model of the losses and the temperature distribution in the transformer with integrated series inductance for optimizing the transformer geometry.

In the following the optimization procedure will be explained briefly. There, also references where the models are explained in detail are listed.

The starting point of the procedure is the initialization of the design parameters like input voltage, output power, temperature limits and material characteristics as presented partially in table I and table II. These parameters as well as starting values like C_S , C_P , L_S , $L_{Out1,2}$ and the number of turns of the transformer (N_P and N_S) must be specified by the user.

With the values for the magnetic components and the turns number the model for the magnetic components is parameterized. There, a reluctance model of the transformer with integrated inductance in combination with the analytical converter model, which describes the operation of the converter and the flux distribution in the core is used in case of the resonant converter [8], [15]. The models for the phase-shift converters are based on analytical expression for the flux distribution and the optimal winding geometry [18].

With the frequency, duty cycle, currents and voltages resulting from the analytical converter model [8], [15], the value and volumes of resonant tank capacitors as well as the switching and conduction losses in the MOSFETs and rectifier diodes are determined, based on the models presented in [8]. These losses, the ambient temperature and the maximum junction temperatures of the semiconductor devices are used for calcu-

lating the volume of the semiconductor heat sink including the fan based on the *CSPI* (Cooling System Performance Index) [17]:

$$CSPI\left[\frac{W}{Kdm^3}\right] = \frac{1}{R_{th,S-a}\left[\frac{K}{W}\right]Vol_{CS}\left[liter\right]} \quad (1)$$

with the thermal resistance $R_{th,S-a}$ of the heat sink and the volume of the heat sink including fan Vol_{CS} .

The volume and the shape of the transformer/inductor core and the two windings is determined in a second, inner optimization procedure, based on a transformer model as presented in [8], [15]. There, the volume of the transformer/inductor is minimized while keeping the temperatures below the allowed limits. The temperature distribution in the core/winding is calculated with a thermal model and the core and the winding losses (including HF-losses).

The resulting minimized transformer/inductor volume are passed to the global optimization algorithm together with the volumes of the heat sink and capacitors. Based on the result the free parameter values are systematically varied until a minimal system volume and/or maximal efficiency is obtained.

More detailed information about the optimization and the corresponding models can be found in [1], [8], [12], [15]

IV. OPTIMIZATION AND SIMULATION RESULTS

Based on the optimization procedure presented in the preceding section the three considered topologies – phase shift with capacitive output filter and current doubler as well as the resonant converter with capacitive output filter – have been optimized for the data given in table I and II. The resulting operating parameters are presented in table III.

The highest power density is achieved with the series-parallel resonant converter: 19.1 kW/ltr. (313 W/in³) if only the net component volumes, the PCBs and housings are considered. The final system volume strongly depends on the 3D design of the converter. For the prototype shown in Fig. 1 the power density resulting of the optimization was 15 kW/ltr., which is lower than the results presented here since other components have been used during the optimization of this converter. The final assembled converter had 10 kW/ltr. (164 W/in³), what results in a scaling factor of 2/3 between calculated and final power density.

The phase-shift converters achieve a power densities of 14.7 kW/ltr. (with current doubler) and 11.7 kW/ltr. (with capacitive output filter). If the scaling factor is assumed as for the assembled resonant prototype, the total system power density of the presented resonant converter is 12.7 kW/ltr. (208 W/in³), for the phase-shift converter with current doubler 7.8 kW/ltr.(128 W/in³) and with capacitive output filter 10 kW/ltr. (164 W/in³).

At the operation point, optimized for maximum power density, the efficiency of the resonant converter is 96.2 %, for the phase shift converter with current doubler 94.8 % and with capacitive output 95.0 % respectively. However, an optimum efficiency results in different switching frequencies for all three converters, as shown in Fig. 4. For the resonant converter the efficiency increases to 96.3 % with an increased switching frequency (≈ 220 kHz), because there, the losses of the

transformer are lower. The phase-shift converter achieves the maximum efficiency when operating with ≈ 100 kHz mainly driven by the decreasing losses of the semiconductors which drastically increase above 300 kHz. A similar behavior shows the phase shift converter with the capacitive output filter. There, the losses becomes minimum at the lowest considered frequency of 25 kHz. However, with the increasing efficiency of the phase shift converter at lower switching frequencies the volume of the magnetic components(transformer and inductor) increases significantly, which results in much smaller power density as shown in Fig. 4.

The dimensions of the ferrite cores (EPCOS N87) are also included in table III and illustrated in Fig. 5. In the optimization of the magnetic devices and foil windings, where only one turn per layer is realized, have been assumed. Moreover, the integration of the required series/leakage inductance for the three converters in the transformer is considered in the

Table III: Resulting operation point and specifications of the optimized 5 kW telecom supplies. There, the losses in the two inductors of the CDR are 2×10.9 W, the AC flux density is 77 mT and the geometry cf. Fig. 5 is: a=10 mm b=21 mm c=7 mm d=12. (In brackets: simulated values including more parasitic elements than considered in the analytic model if differing from the calculated results.)

	Phase Shift		Resonant
	CDR	CTC	SPR-C
Power Density	11.7 kW/ltr.	14.7 kW/ltr.	19.1 kW/ltr.
Operating Point			
• Frequency	200 kHz	100 kHz	135(130) kHz
• Duty Cycle	0.81(0.86)	0.82(0.88)	0.78(0.83)
• Efficiency	94.8 %	95.0 %	96.2 %
Transformer			
• Pri. Wind. Losses	6.0 W	13.0 W	5.7 W
• Sec. Wind. Losses	10.0 W	11.6 W	15.3 W
• Core Losses	13.8 W	23.7 W	23.5 W
• Turns Ratio	11:4	11:2:2	14:2:2
• Winding Temp.	125 °C	124 °C	125 °C
• Core Temp.	107 °C	115 °C	115 °C
• Flux Density	175 mT	240 mT	300 mT
Geometry (cf. Fig.5)			
• Mid Leg a	13.0 mm	15.0 mm	14.0 mm
• Height b	19.3 mm	21.0 mm	12.2 mm
• Window Width c	9.4 mm	7.0 mm	7.0 mm
• Window Height d	15.1 mm	29.4 mm	31.0 mm
• Leakage Leg e	-	7.4 mm	10.6 mm
MOSFETs (cf. Fig. 6)			
• Turn-off current	21.0 A	17.3 A	0 A
$I_{off,A}$	(21.2 A)	(17.7 A)	(≈ 0 A)
• Turn-off current	21.9 A	32.5 A	15.6 A
$I_{off,B}$	(22.2 A)	(31.9 A)	(15.4 A)
• $P_{V,switching}$	31.2 W	17.8 W	<5 W
• $P_{V,conduction}$	93.7 W	96.8 W	64.0 W
L and C			
• Ser. Ind. L_S	2 μ H	12.4 μ H	26.5 μ H
• Out. Ind. L_{OUT}	6.7 μ H	-	-
• Ser. Cap. C_S	-	-	98.5 nF
• Par. Cap. C_P	-	-	26.0 nF
• Out. Cap. C_{OUT}	11 μ F	438 μ F	254 μ F

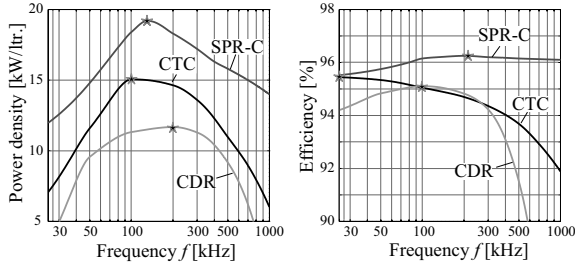


Figure 4: Power density and efficiency of the series-parallel resonant converter with capacitive output (SPR-C), phase-shift converter with current doubler (CDR) and capacitive output (CTC) in dependency of the switching frequency.

optimization. There, also the flux distribution/saturation and HF-losses as skin- and proximity-effect losses are considered. This results, e.g. in an optimal foil thickness of $\approx 65 \mu\text{m}$ for the primary winding and $\approx 150 \mu\text{m}$ for the secondary winding.

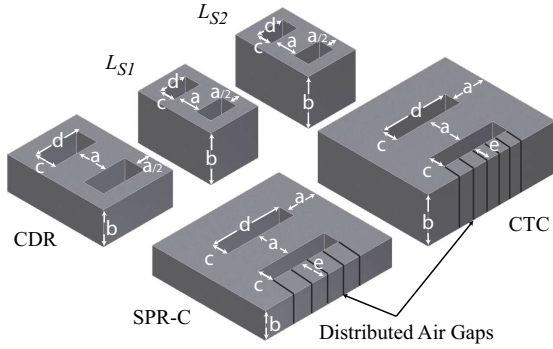


Figure 5: Dimensions of the transformer cores and the inductors (for the CDR) resulting from the optimization procedure for the series-parallel resonant converter with capacitive output (SPR-C), phase-shift converter with current doubler (CDR) and capacitive output (CTC).

A. Simulation Results

With the system parameters resulting from the optimization procedure (cf. table III) simulation models of the converters have been developed in Simplorer (Ansoft). The characteristic simulated waveforms are shown in Fig. 6. The corresponding values resulting from the simulation are given in brackets in table III, where a good correspondence between analytical model and simulation can be seen. The slight differences are caused by the fact, that in the simulation more parasitic elements are considered.

Based on the simulation results, which confirm the analytical optimization, prototypes of the converters can be designed. Some details of these prototypes will be presented in the following section.

V. PROTOTYPES AND MEASUREMENT RESULTS

Based on the optimization results a prototype of the series-parallel resonant converter has been constructed (cf. Fig. 1a and 7).

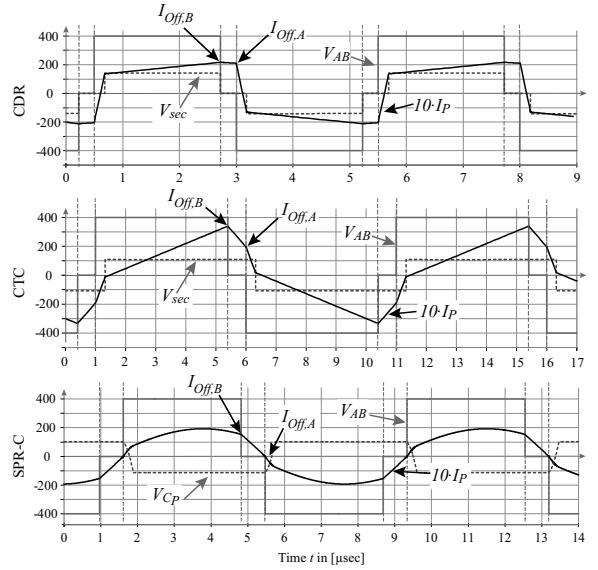


Figure 6: Simulated curves of V_{AB} , I_P , V_{sec} and V_{Cp} (cf. Fig. 1b) and Fig. 2) for the three presented converter with the parameters resulting from the optimization procedure.

This 5 kW prototype has a volume of 0.49 ltr., resulting in a power density of 167 W/in^3 (10.2 kW/ltr.). With the new components utilized in the presented optimization this power density could be increased to approximately 12 kW/ltr.

Besides the optimization of the semiconductor heat sink, the integration of the series inductance L_S and the cooling of the magnetic component is very important. The technical realization of this transformer is illustrated in Fig. 8. The leakage inductance is generated in the top leg by the insertion of distributed air gaps. Since the H-field would result in eddy-currents in the heat transfer component (HTC) of the primary winding/leakage leg, slots are milled into the HTC in the area over the air gaps. Since the primary winding is enclosing the leakage flux path the radiated H-field is relatively low with this design.

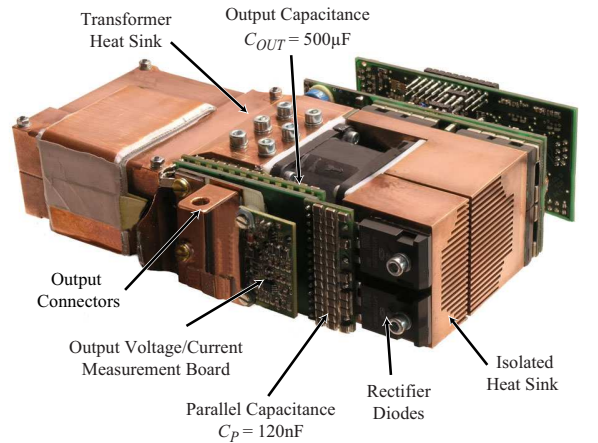


Figure 7: Back view of the resonant DC-DC converter prototype.

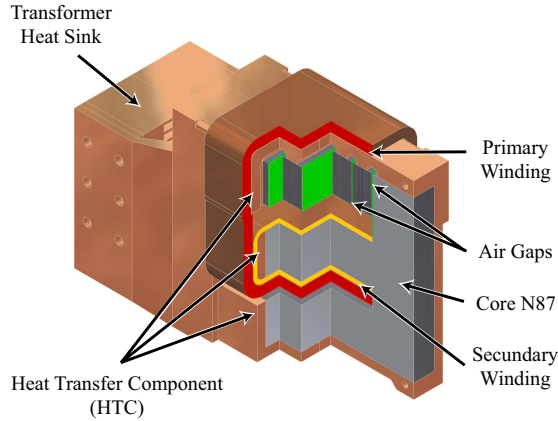


Figure 8: Sectional drawing of the transformer of the resonant converter with integrated series inductance.

In Fig. 9 first measurement results for the resonant converter are shown. There, a nearly sinusoidal waveform of the resonant current at the already maximum designated input voltage of 400 V and the output power of 1.25 kW could be seen.

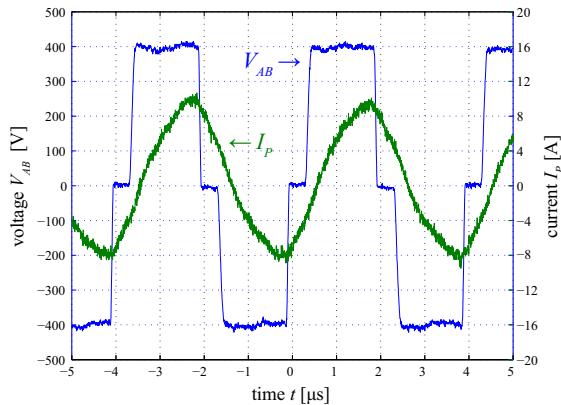


Figure 9: Measurement results of the resonant converter prototype (cf. Fig. 1a)) $V_{IN} = 400$ V, $I_{IN} = 3.4$ A, $V_0 = 44.3$ V, $I_0 = 28.2$ A, $P_O = 1.25$ kW.

A. Copper vs. Aluminum as Heat Sink Materials

In order to obtain the upper limit of the power density, copper has been assumed for the heat sink and the cooling system of the transformer during the optimization. Due to increasing raw material prices the question arises, what is the limit for the power density if aluminum ($\lambda_{Al} = 230$ W/m·K) would be used instead of copper ($\lambda_{Cu} = 390$ W/cm·K).

For determining the impact of the material besides the prototype based on copper also a prototype with aluminum has been designed by numerical CFD simulation (ICEPACK). There the temperature distribution has been kept constant. The different thermal conductivity has a strong influence to the optimal thickness of the fins and the ratio in respect to the air

Table IV: Comparison of heat sink materials: copper and aluminum.

	Copper design	Aluminum design
Heat sink / HTC only	177 cm ³	199 cm ³
Total volume (quader)	499 cm ³	518 cm ³
Power density	10 kW/ltr.	9.65 kW/ltr.

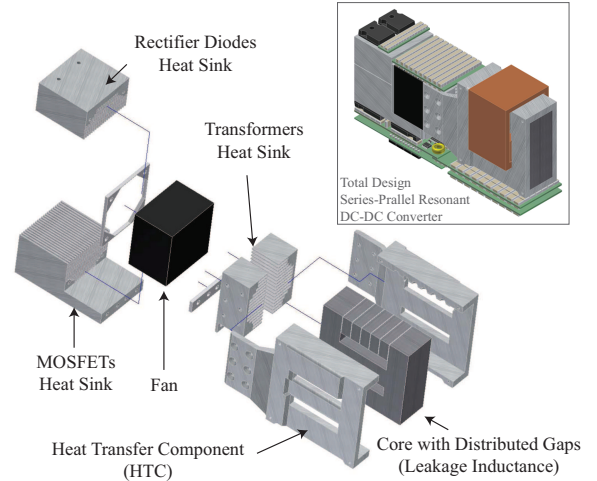


Figure 10: Heat sink components for the series-parallel resonant converter, designed for aluminum.

spaces [17]. By optimizing the design of the fins, the impact of the halved thermal conductivity can be clearly reduced.

The resulting volumes are presented in table IV. The volume of the pure heat sink components (heat transfer components (HTC), heat sink for diodes, MOSFETs and transformer cf. Fig. 10) increases by 9% if copper is replaced by aluminum. However, the total design volume increases only by 3.8%, since . Consequently, the power density decreases by the same factor to 9.65 kW/ltr. Therefore, with a proper design of the air-cool heat sink the overall volume is only slightly influenced by the heat sink material.

B. Integrated Magnetics for the Current Doubler

The optimal volume of the current doubler transformer including core, heat transfer component (HTC), windings and heat sink, is approximately 90 cm³. Together with the two output inductors, the total volume of the magnetic components is approximately 230 cm³ when using very compact commercially available inductors and not considering the space needed for connecting and mounting.

By integrating the output inductors on the same core/winding as the transformer as presented e.g. in [19], [20] the power density can be further increased. With a standard E65/32/27 ferrite core from EPCOS the volume decreases by 6.5% to 215 cm³. With a custom core a reduction of 12% for the volume and also a reduction of the losses in the magnetic devices could be achieved. In Fig. 11 a design of the phase-shift converter with current doubler based on aluminum is shown. There, a power density of approximately 9.75 kW/ltr. could be achieved. This value is higher than the predicted value of 7.8 kW/ltr. due to the integrated magnetics and above

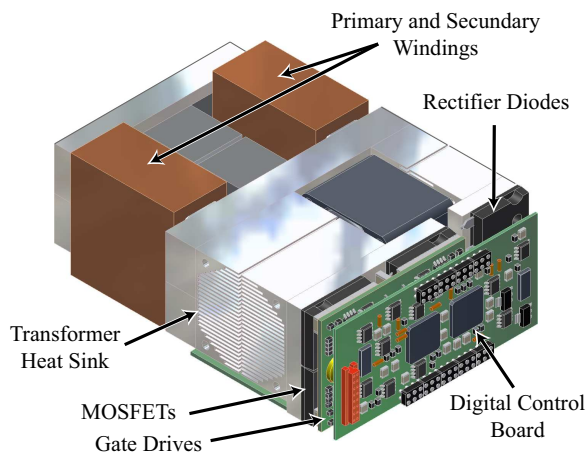


Figure 11: Design of a phase shift converter with current doubler and integrated magnetics. Heat Sinks are made of aluminum.

all due to the more compact design compared to the resonant converter, so that the scaling factor of $2/3$ is increased.

VI. CONCLUSION

In this paper, an optimization procedure is used for maximizing the power density and the efficiency of a phase-shift DC-DC converter with capacitive output filter (CTC) and with current doubler (CDR) as well as a series-parallel resonant with capacitive output filter in order to identify the most suitable topology for 5 kW telecom applications. The analytical models of the optimization procedure include electrical models for the converter, models of the HF losses in the magnetic components, thermal models for the transformer and volume models for the heat sinks/resonant capacitors.

There, maximal 12 kW/ltr., 196 W/in³ (19 kW/ltr. pure component volume) are obtained for the series-parallel resonant converter (SPR). The optimal operating frequency with respect to the power density is approximately 135 kHz. For the phase shift converter 10 kW/ltr. (164 W/in³) result for a capacitive output filter (CTC) and 7.8 kW/ltr. (128 W/in³) for a current doubler (CDR). Again, the optimal operating frequencies are relatively low – approximately 100 kHz for the CTC and 200 kHz for the CDR. There, the efficiencies are 96.2% for the SPR, 95% for the CTC and 94.8% for the CDR. These values slightly improve ($\approx 0.8\%$) if the converter is optimized for efficiency, but there the power density decreases significantly.

By using integrated magnetics for the CDR a volume reduction of 12% for the magnetic components is possible. In case aluminum is used instead of copper for the heat sink and the cooling system of the transformer the system volume increases by approximately 4%.

For validating the analytical models used in the optimization a 5 kW series-parallel resonant DC-DC converter has been constructed and detailed simulations have been performed.

REFERENCES

- [1] J. W. Kolar, U. Drofenik, J. Biela, M. L. Heldwein, H. Ertl, T. Friedli, and S. D. Round, "PWM converter power density barriers," in *Proceedings of the 4th Power Conversion Conference (PCC)*, apr 2007.
- [2] R. L. Steigerwald, R. W. D. Doncker, and M. H. Kheraluwala, "A comparison of high-power dc-dc soft-switched converter topologies," in *IEEE Transactions on Industry Applications*, vol. 32, sep 1996, pp. 1139 – 1145.
- [3] R. Petkov, D. Chapman, and D. James, "A comparative study of two dc/dc converter topologies for telecommunications," in *18th International Telecommunications Energy Conference (INTELEC'96)*. IEEE, oct 1996, pp. 279–288.
- [4] S. Moisseev, S. Hamada, and M. Nakaoka, "Double two-switch forward transformer linked soft-switching PWM dc-dc powerconverter using IGBTs," in *Electric Power Applications, IEE Proceedings*, vol. 150, jan 2003.
- [5] R. Chen, J. T. Strydom, and J. D. van Wyk, "Design of planar integrated passive module for zero-voltage-switched asymmetrical half-bridge PWM converter," in *IEEE transactions on industry applications*, vol. 39, no. 6, nov 2003, pp. 1648–1655.
- [6] B. Yang, F. C. Lee, A. J. Zhang, and G. Huang, "Llc resonant converter for front end dc/dc conversion," in *Applied Power Electronics Conference and Exposition (APEC)*, vol. 2, mar 2002, pp. 1108–1112.
- [7] J. Jacobs, A. Averbeg, S. Schröder, and R. D. Doncker, "Multi-phase series resonant dc-to-dc converters: Transient investigations," in *36th Annual Power Electronics Specialists Conference*, 2005, pp. 1972 – 1978.
- [8] J. Biela, U. Badstübner, and J. W. Kolar, "Design of a 5 kw, 1 u, 10 kw/ltr resonant dc-dc converter for telecomapplications," in *29th International Telecommunications Energy Conference (INTELEC)*, sep 2007.
- [9] A. K. S. Bhat, "A resonant converter suitable for 650 v dc bus operation," in *IEEE Transaction on Power Electronics*, vol. 6, oct 1991, pp. 739–748.
- [10] J. Elek and D. Knurek, "Design of a 200 amp telecom rectifier family using 50 amp dc-dc converters," in *The 21st International Telecommunications Energy Conference (INTELEC)*, jun 1999.
- [11] J. A. Sabate, V. Vlatkovic, R. B. Ridley, F. C. Lee, and B. H. Cho, "Design considerations for high-voltage high-power full-bridge zero-voltage-switched PWM converter," in *Applied Power Electronics Conference and Exposition (APEC)*, mar 1990, pp. 275–284.
- [12] J. W. Kolar, J. Biela, and U. Badstuebner, "Impact of power density maximization on efficiency of dc-dc converter systems," in *The 7th International Conference on Power Electronics (ICPE'07)*, oct 2007.
- [13] T. F. Vescovi and N. C. H. Vun, "A switched-mode 200 a 48 v rectifier/battery charger for telecommunicationsapplications," in *12th International Telecommunications Energy Conference (INTELEC '90)*, 1990, pp. 112–118.
- [14] R. L. Steigerwald, "A comparison of half-bridge resonant converter topologies," in *IEEE Transactions on Power Electronics*, vol. 3, apr 1988, pp. 174 – 182.
- [15] J. Biela and J. W. Kolar, "Analytic model inclusive transformer for resonant converters based on extendedfundamental frequency analysis for resonant converter-design and optimization," in *Transactions of the Institute of Electrical Engineers of Japan (IEEJ)*, ser. 5, vol. 126, 2006, pp. 568 – 577.
- [16] V. Vlatkovic, J. A. Sabate, R. B. Ridley, F. C. Lee, and B. H. Cho, "Small-signal analysis of the phase-shifted PWM converter," in *IEEE Transactions on Power Electronics*, vol. 7, jan 1992, pp. 128–135.
- [17] U. Drofenik, G. Laimer, and J. W. Kolar, "Theoretical converter power density limits for forced convection cooling," in *Proceedings of the International PCIM Europe 2005 Conference*, jun 2005, pp. 608–619.
- [18] W. G. Hurley, E. Gath, and J. D. Breslin, "Optimizing the ac resistance of multilayer transformer windings with arbitrary current waveforms," in *IEEE Transaction on Power Electronics*, vol. 15, no. 2, mar 2000, pp. 369–376.
- [19] H. Zhou, T. X. Wu, I. Batarseh, and K. D. T. Ngo, "Comparative investigation on different topologies of integrated magnetic structures for current-doubler rectifier," in *Power Electronics Specialists Conference PESC 2007*, 2007, pp. 337–342.
- [20] P. Xu, M. Ye, P.-L. Wong, and F. C. Lee, "Design of 48 v voltage regulator modules with a novel integrated magnetics," in *IEEE Transactions on Power Electronics*, vol. 17, no. 6, nov 2002, pp. 990–998.